

DESIGN AND ANALYSIS OF PV SYSTEM WITH Z-SOURCE HALF-BRIDGE CONVERTER

¹ABDUL SHAHID ANSARI, ²Er. DHARMENDRA SINGH

¹SHEPHERD INSTITUTE OF ENGINEERING AND TECHNOLOGY, (SHUATS) ALLAHABAD

²SAM HIGGINBOTTOM UNIVERSITY OF AGRICULTURE, TECHNOLOGY AND SCIENCES

Abstract: In a grid-connected photovoltaic (PV) system, the traditional Z-source inverter uses a low frequency transformer to ensure galvanic isolation between the grid and the PV system. Half bridge converter system is developed for to convert dc power in to the ac and also boost dc output. Due to less no of switches, complicity of converter has been reduced. By adding this Z-source network in between the half bridge converter then this half bridge converter can be also able to operate if duty ratio goes beyond the unity. Conventional half bridge Z-source converter can be used for resistive load. By using the simulation results we can analyze the proposed method. This paper presents a modified single-phase transformerless Z-source PV grid-connected inverter and a corresponding PWM strategy to eliminate the ground leakage current in order to combine the advantages of both Z-source inverters and transformerless PV inverters.

Index Terms—Half-bridge converter, reduced number, shoot-through, Z-source

I. INTRODUCTION

The traditional power converters are basically of two types: voltage-source converters and current source converters. These can be used in single phase as well as three-phase power converters. This paper mainly focuses on a single-phase power conversion. In case of voltage- source (V-source) converters, it acts as a buck (step-down) converter for DC to AC power conversion and as a boost (step-up) converter for AC to DC power conversion. In case of current source (I-source) power converter, it acts as a boost converter for DC to AC power conversion and as a buck converter for AC to DC power conversion. Thus, Vsource and I-source power converter can be used as either as a boost or a buck converter and not as a buck-boost converter.

Moreover, in case of a three-phase power conversion, if both the upper and lower switches of the same leg are simultaneously turned ON either by purpose or by electromagnetic interference, a shoot-through occurs and the converter is damaged. At the past conventional half bridge converter has lots of problem like it cannot produce a broader range of the output voltages and also the shoot-through problem occurs. In conventional half-bridge converter has two switches and they are in one leg as shown in Fig. 1.

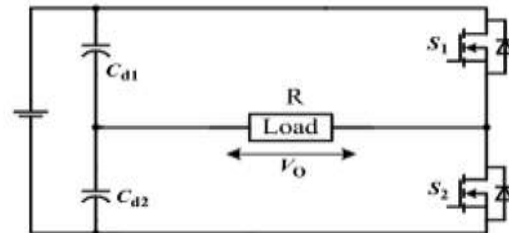


Fig. 1. Conventional half-bridge converter.

If both switches are turn-on at same time the shoot-through problem can occur. Due to this shoot-through problem, large current can flows through these switches, and this makes to short circuits and the switches are getting damage.

The half-bridge inverter output voltage is lower than its source voltage. Furthermore in the conventional half-bridge converter, unbalanced midpoint of split capacitors are makes the system unbalance due to the large ripple.

For the solving of shoot-through phenomenon and limited voltage problem, Peng was proposed the LC network, which is named as the Z-source network as shown in the Fig. 2.

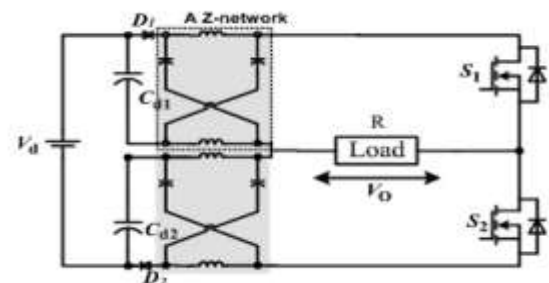


Fig. 2. Z-source half-bridge converter with two Z-networks

The Z-source inverter topology has been significantly modified later. Modified Z-source converter and the control methods have been proposed. New algorithms are proposed to controlling of both AC output voltages and boost DC source of the Z-source converters and dual input and dual output Z-source inverter. Z-source topology is used for lots of applications like a fuel cell system which is proposed.

The Z-source converter has ability to work in the shoot through phenomenon, and the output voltage of the Z-source converter has broader ranges

than that of conventional half bridge converter. Many topologies were developed for the PV applications like a half-bridge converter and full-bridge converter. Conventional half-bridge converters have their switches in series, as shown in Fig. 1, with which the shoot-through can occur, which means that the strong current flowing through the switches makes them break down. Moreover, the ac output voltage is limited below the dc voltage, which is named the limited voltage problem, because, in practice, ac output voltage is sometimes desirable to be higher than the dc voltage. Furthermore, an unbalanced midpoint of input capacitors in conventional half-bridge converters leads to large ripples making the system unstable.

Electroplating is a kind of electrochemical process, whose fundamental operation diagram and operation principle are shown in Fig. 3 and described in the following.

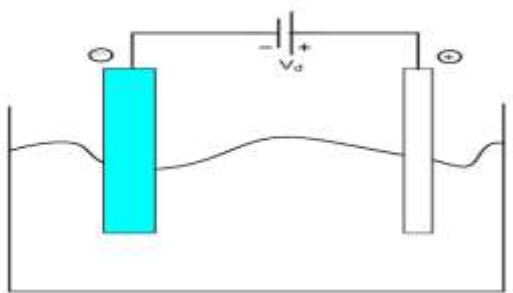


Fig. 3. Diagram of electroplating

The electroplating process is a redox reaction, with fundamental components: two electrodes (+and-), a dc source (V_d), and the solution, as shown in Fig.3. The purpose of the electroplating is to make the metal ions cover the surface of the negative electrode evenly and smoothly. However, due to the non uniformity of the solution, the dc-voltage direction and the current density should be changed from time to time, which requires complicated designs according to different products and processes. With the rapid growth of the demand on electroplating products with very different voltages and duties, there are more stringent requirements on the electrochemical power supplies to provide a broad range of outputs, asymmetrical positive and negative voltages, step waves, recurrent pulses, square waves, triangular waves, and saw-tooth waves which can be quite well fulfilled by the proposed converter.

II. SYSTEM DESIGN AND ANALYSIS

The proposed converter is depicted in Fig. 4, in which an LC Z-network, consisting of capacitors C_1 and C_2 and inductors L_1 and L_2 , is integrated into a traditional half-bridge converter, consisting of capacitors C_{d1} and C_{d2} , switches S_1 and S_2 , and diode D , which is used to prevent the current from flowing back to the source. Therein, the use of the inductors in the Z-network is to avoid

strong current in the circuit when the switches are in the shoot-through state

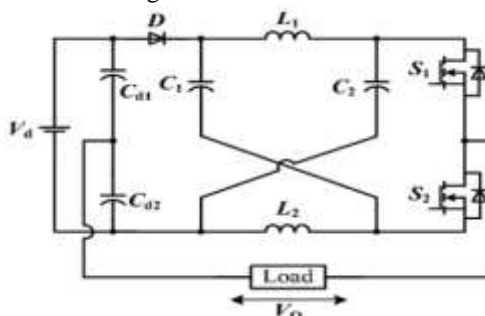


Fig. 4. Z-source half-bridge converter

For simplicity, the following conditions are assumed: 1) All the components are ideal; 2) the dead time in the driven pulses is ignored; 3) $L_1=L_2$ and $C_1=C_2$ in the Z-network; 4) C_1, C_2, C_{d1} , and C_{d2} are large enough; and 5) the free-wheeling diodes of the switches are ignored in the analysis since the load characteristic of the electrochemical solution is resistance or resistance with a small capacitance. Denote the duties of the switches S_1 and S_2 by D_1 and D_2 , respectively. The proposed converter performs differently in two cases: $D_1+D_2 \leq 1$ and $D_1+D_2 > 1$.

A. Case 1: $D_1+D_2 \leq 1$

In this case, S_1 and S_2 are not switched on at the same time; then, the circuit is in the non-shoot-through state. There are three modes corresponding to the states of the switches.

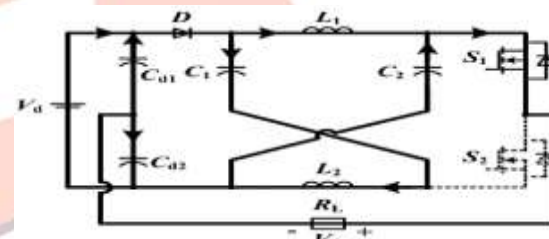


Fig. 5. Equivalent circuits in case 1. (a) S_1 on and S_2 off.

In the first mode, Fig. 5(a) shows an equivalent circuit for the mode when the S_1 is on and S_2 is off, in which the current flows out of the source, through the diode, the Z-network, and S_1 , and then back to the source. The arrows indicate the current directions.

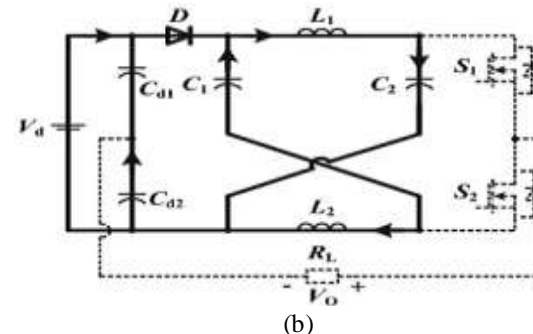


Fig. 5. Equivalent circuits in case 1. (a) S_1 on and S_2 off. (b) S_1 off and S_2 on.

In the second mode, Fig. 5(b) shows an equivalent circuit of that when S_1 and S_2 are off, in which the current also flows out of the source, through the diode and the Z-network, and back to the source; there is no output here. In the third mode, Fig. 5(c) shows an equivalent circuit of that when S_2 is on and S_1 is off, in which the diode suffers a negative voltage and, thus, turns off. The current flows out of the source, through the load, S_2 , and the Z-network, and then back to the source. Furthermore, the current direction is also indicated. The operation process for this case is similar to the traditional one for half-bridge converters, which is not detailed here.

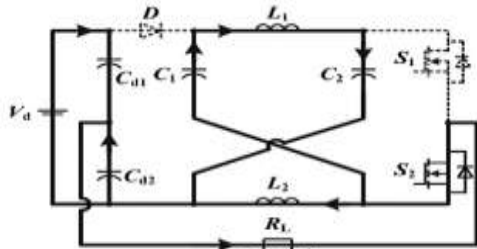


Fig. 5. Equivalent circuits in case 1. (a) S_1 on and S_2 off. (b) S_1 off and S_2 off. (c) S_1 off and S_2 on
B. Case 2: $D_1 + D_2 > 1$

In this case, the behavior of the switches in the circuit leads to three modes within a switch period T , which correspond to three linear equivalent circuits: Mode 1, when S_1 and S_2 are on; Mode 2, when S_1 is on and S_2 is off; and Mode 3, when S_1 is off and S_2 is on, as shown in Fig. 6(a)–(c), respectively.

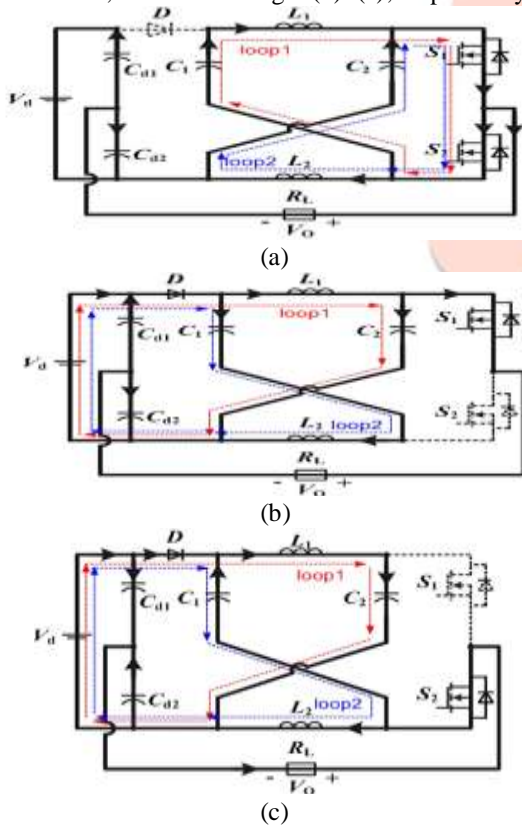


Fig. 6. Equivalent circuits in case 2. (a) Mode 1: S_1 on and S_2 on. (b) Mode 2: S_1 on and S_2 off. (c) Mode 3: S_1 off and S_2 on.

In the steady state of the converter, its operation process in a switch period is analyzed in the following, and the output voltage v_o will be deduced in each mode.

1) Mode 1: $t \in [t_0, t_1]$: As shown in Fig. 6(a), in loops 1 and 2, capacitors C_1 and C_2 discharge the energy to inductors L_1 and L_2 ; thereafter, i_{L1} and i_{L2} increase. Thus, L_1 and L_2 store the energy, and one has

$$\begin{cases} v_{L1} = v_{C1} \\ v_{L2} = v_{C2} \end{cases} \quad (1)$$

where i_{L1} , i_{L2} , v_{L1} , v_{L2} , v_{C1} , and v_{C2} are the currents of L_1 and L_2 and the voltages of L_1 , L_2 , C_1 , and C_2 , respectively. The voltage of diode D is $-(v_{C1} + v_{C2} - V_d)$, so D undertakes negative voltage stress and, thus, turns off. The energy of C_2 is delivered to the load R_L and C_{d2} through the C_2 - R_L - C_{d2} loop, so C_{d2} charges and C_{d1} discharges. In terms of the C_2 - R_L - C_{d2} loop, the output voltage of the converter reads

$$v_o = v_{C2} - v_{C_{d2}} \quad (2)$$

where $v_{C_{d2}}$ is the voltage of C_{d2} . 2) Mode 2: $t \in [t_1, t_2]$: As shown in Fig. 6(b), S_1 is on, and S_2 is off. In loop 1, the source V_d and L_1 discharge the energy to C_2 , so that v_{C2} increases. In loop 2, the source V_d and L_2 discharge the energy to C_1 ; thereafter, v_{C1} increases. Then, the energy of C_2 is delivered to the load R_L and C_{d2} through the C_2 - R_L - C_{d2} loop, so C_{d2} charges and C_{d1} discharges. From loop 1, one has

$$v_{L1} = V_d - v_{C2} \quad (3)$$

In terms of the C_2 - R_L - C_{d2} loop, the output voltage of the converter is the same as that in (2).

Mode 3: $t \in [t_2, t_3]$: In Fig. 6(c), S_1 is off, and S_2 is on. In loop 1, the source V_d and L_1 discharge the energy to C_2 ; thus, v_{C2} increases. In terms of loop 1, one has the same equation as (3). In terms of the V_d - D - C_1 - R_L - C_{d2} loop, the output voltage is

$$v_o = -(v_{C_{d2}} + v_{C2} - V_d) \quad (4)$$

As a result, v_o can be deduced as follows. The voltage-second characteristic of L_1 leads to

$$\int_0^T v_{L1} dt = 0 \quad (5)$$

Substituting (1) and (3) into (5) leads to $(D_2 + D_1 - 1)T v_{C1} + (2 - D_2 - D_1)T(V_d - v_{C2}) = 0$

Assume that $L_1 = L_2$, $C_1 = C_2$, and C_1 and C_2 are large enough. Due to the structural symmetry of the Z-network, (6) can be rewritten as

$$v_{C1} \approx v_{C2} = \frac{2 - D_1 - D_2}{3 - (D_1 + D_2)} V_d \quad (7)$$

The ampere-second property of C_{d2} implies that $\int_0^T i_{C_{d2}} dt = 0$

where $i_{C_{d2}}$ is the current of C_{d2} . Denote the voltage and current of C_{d1} by $v_{C_{d1}}$ and $i_{C_{d1}}$

,respectively. It is known from Fig. 6 that $v_{Cd1}+v_{Cd2}=V_d$. Due to V_d being a constant, one has $\Delta v_{Cd1}=-\Delta v_{Cd2}$, and straightforwardly, $i_{Cd1}=i_{Cd2}$ in terms of $i=Cdu/dt$. Moreover, from $i_o=i_{Cd1}+i_{Cd2}$, one has $i_{Cd2}=i_o/2$ where i_o is the current of the load; thereafter, (8) can be rewritten as

$$\frac{(v_{C2}-v_{Cd2})}{2R_L} D_1 T + \frac{-(v_{C2}+v_{Cd2}-V_d)}{2R_L} (1-D_1) T = 0 \quad (9)$$

and it follows that

$$v_{Cd2} = (2v_{C2} - V_d) D_1 - v_{C2} + V_d \quad (10)$$

When switch S_1 is on, substituting (7) and (10) into (2) results in the positive output of the converter as

$$v_p = v_o = v_{C2} - v_{Cd2} = \frac{(1-D_1)}{3-2(D_1+D_2)} V_d \quad (11)$$

When the switch S_2 is on and S_1 is off, substituting (7) and (10) into (4) leads to the negative output of the converter as

$$v_n = v_o = v_d - v_{C2} - v_{Cd2} = -\frac{D_1}{3-2(D_1+D_2)} V_d \quad (12)$$

According to (11) and (12), the relationships of D_1 , D_2 , and v_o/V_d are drawn in Fig. 7.

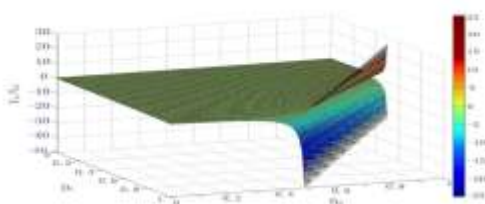


Fig. 7. Relationship figure of D_1, D_2 , and v_o/V_d

There in, v_o/V_d increases dramatically as D_1+D_2 is about 1.5, which is zoomed in in Fig. 8. When $v_o/V_d < 1$, the converter functions as a buck converter; otherwise, the converter acts as a boost converter.

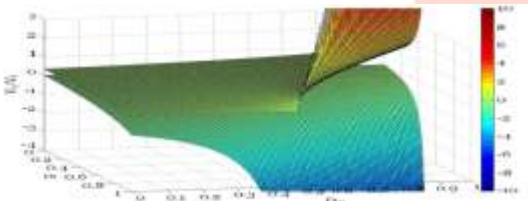


Fig. 8. Zooming in of Fig. 7.

Therefore, it is a buck-boost converter. By controlling the duty of the switches, special output voltages can be obtained, including the buck-boost voltages, asymmetric and symmetric voltages, positive and negative peak output voltages, and the time ratio between positive and negative voltages.

Additionally, according to (11) and (12), the values of v_p and v_n are not equal when $D_1=0.5$, but they are equal when $D_1=0.5$, which will be explained hereinafter. First, when $D_1=0.5$, the key waveforms of the Z-source half-bridge converter in case 2 are drawn in Fig. 9

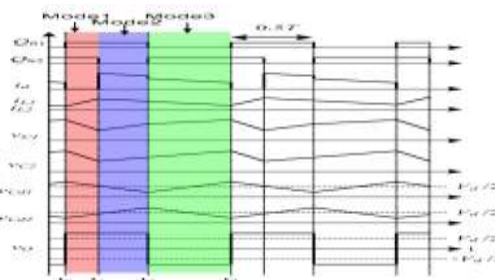


Fig. 9. Key waveforms of the Z-source half-bridge converter in case 2 when $D_1=0.5$ and $D_2=0.7$

According to the analysis for three modes, where Q_{S1} and Q_{S2} stand for the driving voltages of switches S_1 and S_2 , respectively $V_d/2$ and $-V_d/2$ are marked at the output voltage waveform v_o , and it is shown that the output voltages of the proposed converter can exceed the limited one. Second, the corresponding waveforms for $D_1=0.5$ are shown in Fig. 10. Here, the conduction and switching loss is taken into account, which is indicated in Pin - Pout.

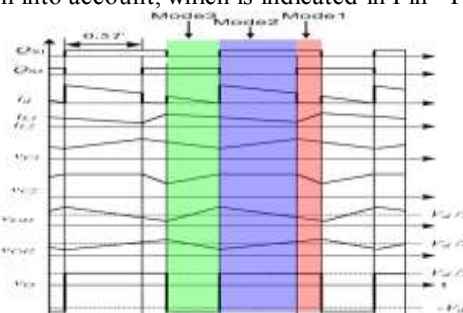


Fig. 10. Waveforms of the Z-source half-bridge converter in case 2 when $D_1=0.7$ and $D_2=0.5$

III. MIDPOINT BALANCE OF INPUT CAPACITORS

The stability of the midpoint voltage in the converter plays a key role for the system's stability. The midpoint voltages of the input capacitors in the conventional converter and the proposed converter will be analyzed and compared in this section.

A. Midpoint Voltage in Conventional Half-Bridge Converters

In this section, the midpoint voltage in conventional half-bridge converters will be analyzed, and the fluctuation equation of the midpoint voltage will be deduced. Fig. 11 shows the equivalent circuits of that in Fig. 1.

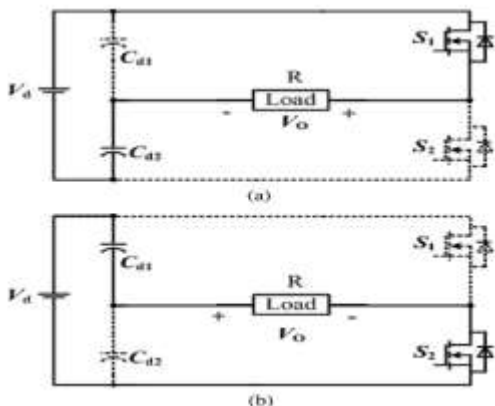


Fig. 11. Equivalent circuits of the conventional half-bridge converter. (a) Mode 1: S1 on and S2 off. (b) Mode 2: S1 off and S2 on.

In a switching period, S1 is on and S2 is off as \$t \in [0, D1T]\$, while S1 is off and S2 is on as \$t \in [D1T, T]\$. Denote the initial voltage of \$C_{d2}\$ by \$V_{Cd20}\$. In terms of the Kirchhoff's voltage law (KVL), \$v_{Cd2}\$ can be derived in frequency domain as

$$v_{Cd2}(s) = \frac{V_d}{s} - \frac{V_d - v_{Cd20}}{s + \frac{1}{C_{d2}R}} \quad (13)$$

Employing Laplace inverse transformation to (14) results in

$$v_{Cd2}(t) = V_d - (V_d - v_{Cd20})e^{-\frac{t}{C_{d2}R}} \quad (14)$$

Denote the maximal and the minimal voltages of \$v_{Cd2}\$ by \$v_{Cd2max}\$ and \$v_{Cd2min}\$, respectively, and the maximal fluctuation of \$v_{Cd2}\$ by \$\Delta V\$. Following (15), one has

$$\Delta V = v_{Cd2max} - v_{Cd2min} = (V_d - v_{Cd20}) \left(1 - e^{-\frac{D1T}{C_{d2}R}}\right) \quad (15)$$

In the high-frequency power supply, T is always very small, the input capacitance \$C_{d2}\$ is always quite large, particularly in electrochemical application, and its load is very large. Thus, \$D1T\$ is much smaller than \$C_{d2}R\$, and (16) can be approximated by

$$\Delta V \approx \frac{D1T}{C_{d2}R} (V_d - v_{Cd20}) \quad (16)$$

B. Midpoint Voltage in Z-Source Half-Bridge Converters

It is described in [29] that the input part can be regarded as a dc voltage source or a dc current source due to the Z-network. Similarly, the output part of the Z-network can be treated as a dc current source. Hence, the equivalent circuits are derived as follows. The differential equation of the circuit shown in Fig. 12(a) can be described as

$$C_{d2} \frac{dv_{Cd2}}{dt} = I_p \quad (17)$$

where \$I_p\$ is the current of the constant current source. Integrating both sides of (18) leads to

$$v_{Cd2}(t) = v_{Cd20} + \int \frac{I_p}{C_{d2}} dt \quad (18)$$

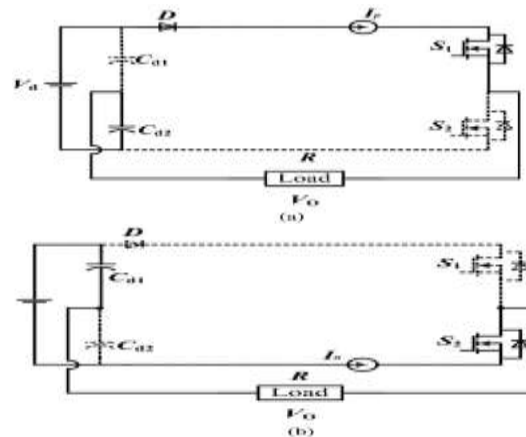


Fig. 12. Equivalent circuits of the Z-source half-bridge converter. (a) Mode 1: S1 on and S2 off. (b) Mode 2: S1 off and S2 on.

\$I_p\$ can be derived by Kirchhoff's current law (KCL) as

$$I_p = \frac{V_d - v_{Cd20} - V_{ip}}{R} \quad (19)$$

Where \$V_{ip}\$ is the voltage of the constant current source. Substituting (21) into (20) leads to

$$\Delta V_Z = D_1 T \frac{V_d - v_{Cd20} - V_{ip}}{C_{d2}R} \quad (20)$$

Therein, the ratio of \$\Delta V_Z\$ to \$\Delta V\$ can be derived from (17) and (22) as

$$\frac{\Delta V_Z}{\Delta V} = \frac{V_d - v_{Cd20} - V_{ip}}{V_d - v_{Cd20}} * 100\% \quad (21)$$

It is obvious that \$\Delta V_Z < \Delta V\$, if \$V_{ip}\$ is positive; the smaller the \$\Delta V_Z/\Delta V\$ is, the smaller the ripple in the proposed converter is and, consequently, the more stable the proposed converter is.

IV. PARAMETER DESIGN

The parameters of the Z-network are designed in this section, including capacitor and inductance parameter design.

A. Parameter Design of the Capacitor in the Z-Network

Normally, the design of the capacitor is to determine the rated voltage and capacitance with a permitted fluctuation range \$x\%\$ (\$x\$ is preassigned), a given output voltage \$V_o\$, a given output current \$I_o\$, and a given switching period T. From (7), (11), and (12), one has

$$v_{C2} = \frac{2-D_1-D_2}{D_1} V_o \quad \text{when } (S_1)=(\text{on}) \quad (22)$$

$$v_{C2} = \frac{2-D_1-D_2}{1-D_1} V_o \quad \text{when } (S_1, S_2)=(\text{off}, \text{on}) \quad (23)$$

Denote the rms currents of \$L_2\$ and \$C_2\$ by \$I_{L2}\$ and \$I_{C2}\$, respectively. Then, from (24), one has

$$I_{C2} \approx I_{L2} = \frac{I_o}{2} \quad (24)$$

1) Determination of the Rated Voltage: The range of \$v_{C2}\$ is determined by (24) and (25). Thereby, the rated voltage of \$C_2\$ can be determined by the maximal \$V_{C2M}\$. Considering the safety margin, the rated voltage of \$C_2\$ is normally set between \$1.5V_{C2M}\$ and \$2V_{C2M}\$.

2) Determination of the Rated Capacitance: The ripples of the capacitors have great influence on the

stability of the converter, whose permitted fluctuation range can be used to design the capacitance.

The high harmonic frequency of the capacitance is nearly equal to the switching frequency of the converter, as shown in Fig. 9, namely,

$$dt \approx (D_1 + D_2 - 1)T \tag{25}$$

Denote the permitted error of V_{C2} by ΔV_{C2} , according to the permitted fluctuation range ΔV_{C2} , ΔV_{C2} is expressed as

$$\Delta V_{C2} = xC\% V_{C2} M \tag{26}$$

Substituting (27), (29), and (30) into (28) leads to

$$C_2 = \frac{I_0 (D_1 + D_2 - 1) T}{2xC\% V_{C2} M} \tag{27}$$

B. Parameter Design of the Inductor in the Z-Network

Similar to the parameter design of the capacitor, the parameter design of the inductor is to determine the rated current and capacitance with a permitted fluctuation range $xL\%$ (xL is pre assigned), a given output voltage V_o , a given output current I_o , and a given switching period.

1) Determination of the Rated Current: I_{L2} can be determined by (27). Considering the safety margin, the rated current of L_2 is normally taken as $2I_{L2}$

2) Determination of the Rated Inductance: The ripples of the inductors also have great influence on the stability of the converter; therefore, the inductance can be designed in terms of the permitted ripples. The inductances in the Z-network can be designed according to the differential equation of inductance

$$L_2 = \frac{V_{L2} dt}{di L_2} \tag{28}$$

In the $L_1-C_2-L_2-C_1$ loop, the KVL equation can be expressed as $V_{L2} + V_{C1} = V_{L1} + V_{C2}$ so the Z-network, the rms voltages of C_1 , C_2 , L_1 , and L_2 are denoted by V_{C1} , V_{C2} , V_{L1} , and V_{L2} , respectively, and one has $V_{C1} \approx V_{C2}$ and $V_{L2} \approx V_{L1}$. Thereby, the maximum of V_{L2} is derived a

$$V_{L2M} \approx V_{C2M} \tag{29}$$

Denote the permitted error of I_{L2} by ΔI_{L2} . According to the permitted fluctuation range ΔI_{L2} , ΔI_{L2} is expressed as

$$\Delta I_{L2} = \frac{2V_{C2M} (D_1 + D_2 - 1) T}{xL\% I_0} \tag{30}$$

Substituting (24), (25), (27), and (33)–(35) into (32) leads to the inductance of L_2

$$L_2 = xL\% I_{L2} \tag{31}$$

PV SOURCE

Photovoltaics (PV) covers the conversion of light into electricity using semiconducting materials that exhibit the photovoltaic effect, a phenomenon studied in physics, photochemistry, and electrochemistry. The dynamic model of PV cell is shown in below Fig.13.

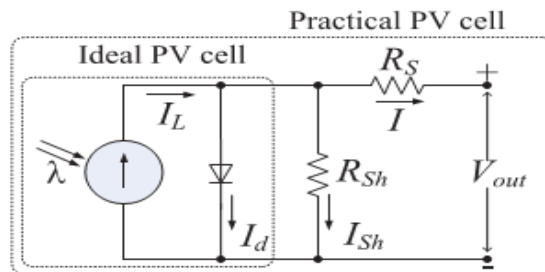


Fig 13. Equivalent electrical circuit of the PV cell. The basic equation describing the I - V characteristic of a practical PV cell is

$$I = I_L - I_d - I_{sh} = I_L - I_D \left[e^{\frac{QV_{oc}}{AKT}} - 1 \right] - \frac{V_{out} + IR_s}{R_{sh}} \tag{27}$$

where I_D is the saturation current of the diode, Q is the electron charge, A is the curve fitting constant (or diode emission factor), K is the Boltzmann constant and T is the temperature on absolute scale.

V. SIMULATION RESULTS

To verify the feasibility and validity of the proposed converter, Simulink software is applied for the simulation of the converter. The pre assigned parameters are as follows: $xC\% = 1\%$, $xL\% = 10\%$, $V_d = 48V$, $V_o = 100V$, $I_o = 10A$, and $T = 20\mu s$. According to the design, the parameters of the converter can be calculated: $C_1 = C_2 = 482.5\mu F$ and $L_1 = L_2 = 105.5\mu H$. However, in practice, the parameters can be chosen as follows: $C_1 = C_2 = 470\mu F$ and $L_1 = L_2 = 100\mu H$

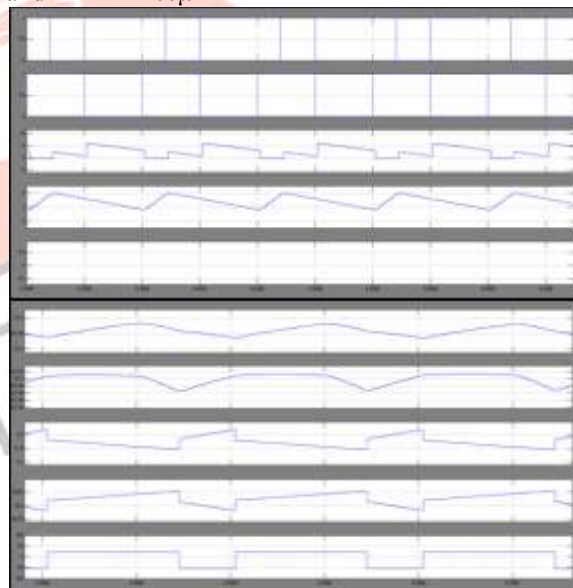


Fig. 14. Simulation waveforms when $D_1 = 0.5$ and $D_2 = 0.7$

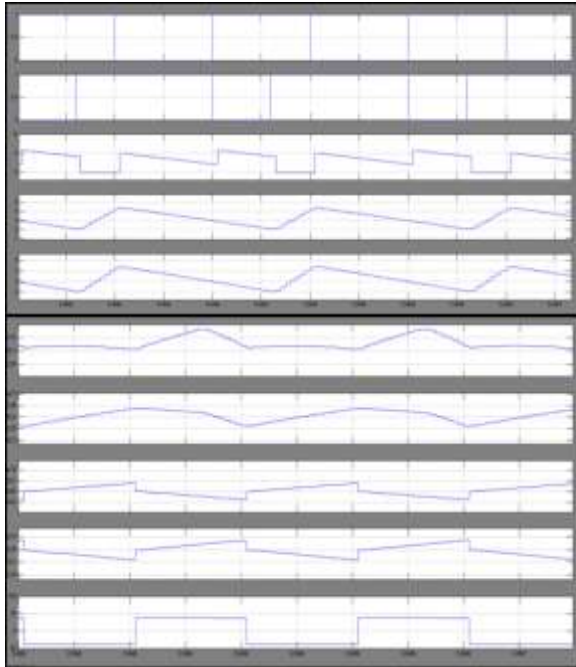


Fig. 15. Simulation waveforms when $D1=0.7$ and $D2=0.5$.

The simulation results are shown in Figs. 13 and 14, which are consistent to the theoretical analyses shown in Figs. 9 and 10.

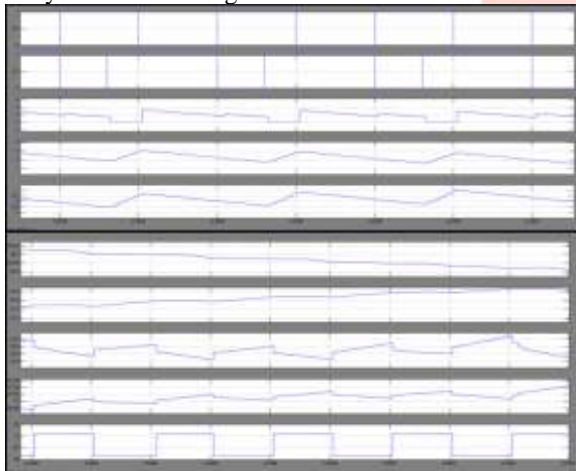


Fig :16 simulation waveform with pv when $D1=0.5$ and $D2=0.7$

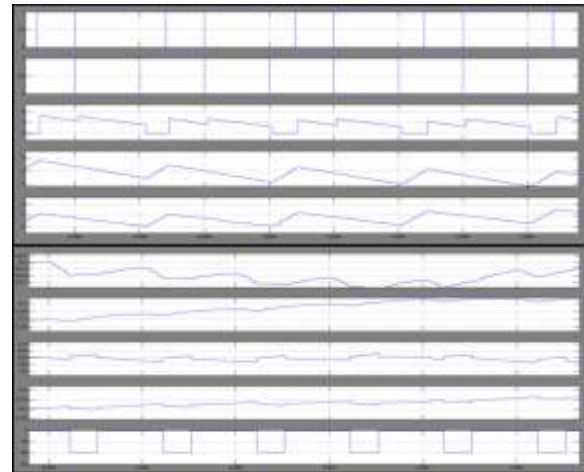


Fig :17 simulation waveform with pv when $D1=0.7$ and $D2=0.5$

VI. CONCLUSION

This paper proposes a Z-source half bridge converter for a photovoltaic application. This paper presents the improved performance of the Z-source half bridge converter. These are the following advantages of existing half bridge converter over the proposed Z-source half bridge converter. 1 Proposed topology can be able to operate for the resistive and the inductive load. 2 Proposed topology also capable for the photovoltaic application. the converter has been analyzed in two different states, including the shoot-through and non-shoot-through states. Furthermore, the feature of the proposed converter owning abundant outputs under an appropriate control is very desirable for requirements of the electrochemical power supply. By using the simulation results we can analyze the proposed method.

REFERENCES

- [1] B. Zhao, Q. G. Yu, Z. W. Leng, and X. Y. Chen, "Switched Z-source isolated bidirectional DC-DC converter and its phase-shifting shoot through bivariate coordinated control strategy," *IEEE Trans. Ind. Electron.*, vol. 59, no. 12, pp. 4657-4670, Dec. 2012.
- [2] Y. C. Hung, F. S. Shyu, C. J. Lin, and Y. S. Lai, "New voltage balance technique for capacitors of symmetrical half-bridge converter with current mode control," in *Proc. PEDS*, 2003, pp. 365-369.
- [3] Z. Liu, B. Liu, S. Duan, Y. Kang, and K. N. J. Soon, "A novel DC capacitor voltage balance control method for cascade multilevel STATCOM," *IEEE Trans. Power Electron.*, vol. 27, no. 1, pp. 14-27, Jan. 2012.
- [4] J. Eloy-Garcia, S. Arnaltes, and J. L. Rodriguez-Amenedo, "Extended direct power control for multilevel inverters including DC link middle point voltage control," *IET Elect. Power Appl.*, vol. 1, no. 4, pp. 571-580, Jul. 2007.
- [5] J. Eloy-Garcia, S. Arnaltes, and J. L. Rodriguez-Amenedo, "Extended direct power control of a three-level neutral point clamped voltage source inverter

with unbalanced voltages,” in Proc. IEEE PESC, 2008, pp. 3396–3400.

[6] T. S. Win, Y. Baba, M. Okamoto, E. Hiraki, and T. Tanaka, “A halfbridge inverter based active power quality compensator with a DC voltage balancer for electrified railways,” in Proc. IEEE PEDS, Dec. 2011, pp. 185–190.

[7] T. Tanaka, K. Ishibashi, N. Ishikura, and E. Hiraki, “A half-bridge inverter based active power quality compensator for electrified railways,” in Proc. Int. Power Electron. Conf., 2010, pp. 1590–1595.

[8] M. Kamli, S. Yamamoto, and M. Abe, “A 50–150 kHz half-bridge inverter for induction heating applications,” IEEE Trans. Ind. Electron., vol. 43, no. 1, pp. 163–172, Feb. 1996.

[9] D. Boroyevich, D. Zhang, and P. Ning, “A shoot-through protection scheme for converters built with SiC JFETs,” IEEE Trans. Ind. Appl., vol. 46, no. 6, pp. 2495–2500, Nov./Dec. 2010.

[10] Z. L. Yao, L. Xiao, and Y. G. Yan, “Strategy for series and parallel output dual-buck half bridge inverters based on DSP control,” IEEE Trans. Power Electron., vol. 24, no. 2, pp. 434–444, Feb. 2009.

[11] F. Z. Peng, “Z-source inverter,” IEEE Trans. Ind. Appl., vol. 39, no. 2, pp. 504–510, Mar./Apr. 2003.

[12] B. M. Ge, Q. Lei, W. Qian, and F. Z. Peng, “A family of Z-source matrix converters,” IEEE Trans. Ind. Electron., vol. 59, no. 1, pp. 35–46, Jan. 20

